Toroidal pores formed by antimicrobial peptides show significant disorder

Durba Sengupta [a,b], Hari Leontiadou [a,b,1], Alan E. Mark [c,d], Siewert-Jan Marrink [a,b,*]

[a] Groningen Biomolecular Sciences and Biotechnology Institute, University of Groningen, Nijenborgh 4, 9747 AG Groningen, The Netherlands
[b] Zernike Institute for Advanced Materials, University of Groningen, Nijenborgh 4, 9727 AG Groningen, The Netherlands
[c] School of Molecular and Microbial Sciences, University of Queensland Brisbane, QLD 4072, Australia
[d] Institute for Molecular Biosciences, University of Queensland Brisbane, QLD 4072, Australia

ARTICLE INFO

ABSTRACT

A large variety of antimicrobial peptides have been shown to act, at least in vitro, by poration of the lipid membrane. The nanometre size of these pores, however, complicates their structural characterization by experimental techniques. Here we use molecular dynamics simulations, to study the interaction of a specific class of antimicrobial peptides, melittin, with a dipalmitoylphosphatidylcholine bilayer in atomic detail. We show that transmembrane pores spontaneously form above a critical peptide to lipid ratio. The lipid molecules bend inwards to form a toroidally shaped pore but with only one or two peptides lining the pore. This is in strong contrast to the traditional models of toroidal pores in which the peptides are assumed to adopt a transmembrane orientation. We find that peptide aggregation, either prior or after binding to the membrane surface, is a prerequisite to pore formation. The presence of a stable helical secondary structure of the peptide, however is not. Furthermore, results obtained with modified peptides point to the importance of electrostatic interactions in the poration process. Removing the charges of the basic amino-acid residues of melittin prevents pore formation. It was also found that in the absence of counter ions pores not only form more rapidly but lead to membrane rupture. The rupture process occurs via a novel recursive poration pathway, which we coin the Droste mechanism.

© 2008 Elsevier B.V. All rights reserved.

1. Introduction

Antimicrobial peptides (AMPs) are an integral part of the innate immune system of higher organisms [1]. These host defense peptides possess a wide spectrum of antimicrobial activity against eubacteria, fungi, viruses and eukaryotic parasites [2]. The development of resistance by pathogens against traditional antibiotics has triggered much interest in AMPs, both from a basic scientific perspective, and because of their potential applications in biotechnology. To design synthetic AMP-like pharmaceuticals it is necessary to know the molecular details involved in the modes of actions of natural AMPs. AMPs have both receptor-mediated and nonreceptor-mediated modes of action [1,3]. The most abundant of the nonreceptor-mediated peptides are the small cationic peptides that target negatively-charged bacterial membranes [2]. In general, such small AMPs bind to the surface of the membrane until a critical threshold concentration is reached, after which they self-organize to form a permeation pathway. Pore formation has been proposed to occur via a variety of mechanisms [1,2,4,5] as shown in Fig. 1 and described below.

Outside the target membrane, peptide monomers and small aggregates exist in equilibrium [6,7]. In solution the peptides are believed to be largely unfolded [1,8] (Fig. 1). At the target membrane, the peptides bind to the interface and fold. At low peptide concentrations, most peptides are believed to bind parallel to the membrane surface and may be monomeric or aggregated [1]. Above a certain peptide/lipid ratio, a transmembrane pore appears associated with the peptides adopting a more perpendicular orientation [1,4]. Peptides such as alamethicin insert into the bilayer to form a barrel-stave pore structure [9]. Other peptides, such as the magainins and melittins, induce local defects in the bilayer and form a toroidal pore [10,11]. In this case, the head-groups of the lipids line the pore together with the peptides. An increase in the local accumulation of certain peptides such as melittin may also lead to a detergent-like disintegration of the bilayer structure via a carpet mechanism [12], resulting in the formation of micellar or bicellar aggregates. Alternatively, the translocation of peptides across the membrane may restore the balance between the two bilayer leaflets leading to pore closure, as proposed in the sinking-raft model [13]. It is also possible that peptides adsorbed to the surface may translocate across the membrane without forming a pore. To truly understand pore formation, one must be able to distinguish between the thermodynamically stable or metastable states, such as the bilayer and toroidal pore states, and the kinetic pathways, such as the toroidal and carpet mechanisms, that connect them.
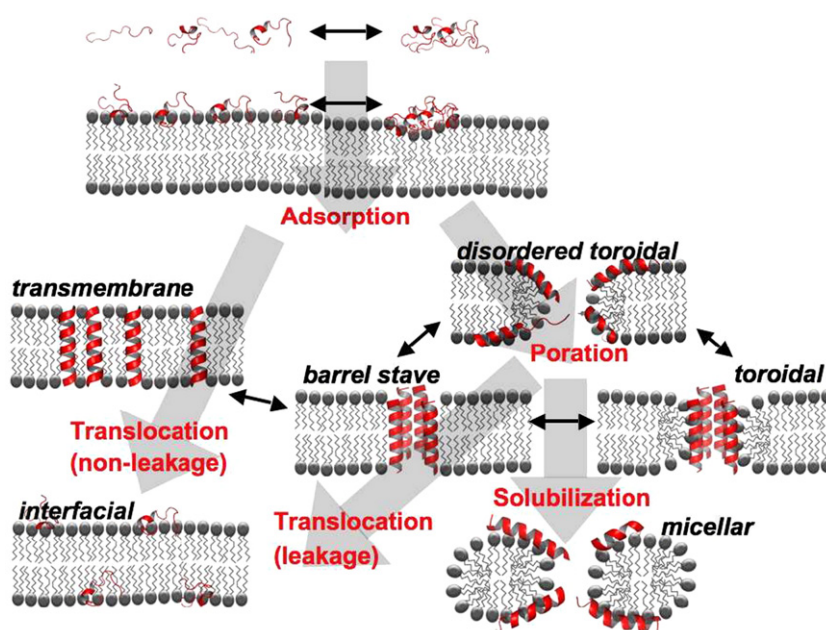
Fig. 1. Schematic overview of the possible interaction pathways of an antimicrobial peptide with a lipid bilayer. Possible thermodynamic states (either stable or metastable) are indicated by black labels, the major kinetic pathways connecting them by gray arrows and red labels. Short black arrows represent additional inter-conversion pathways. Outside the target membrane, peptide monomers and small aggregates exist in equilibrium. At the target membrane, the peptides bind to the interface (Adsorption). At the interface an equilibrium may exist between monomeric and polymeric aggregation states. For a symmetric bilayer, the asymmetric membrane bound state is not thermodynamically stable. Eventually the peptides will distribute equally between the two monolayer leaflets. This can occur via two alternative translocation pathways. In the non-leaky variant the peptides are able to cross the bilayer without the formation of a pore. In some cases, the intermediate transmembrane state is thermodynamically stable (e.g. hydrophobic peptides which adopt a transmembrane orientation). The key feature of many antimicrobial peptides is that they permeabilize the membrane following a leaky translocation pathway. Above a certain peptide–lipid ratio, the peptides insert into the bilayer to form a porated lamellar phase (Poration). A variety of different pore structures may be formed, including the barrel-stave, the toroidal and the disordered toroidal state. These separate states should be interpreted as extreme cases with mixed varieties of these models, and conversion between alternative states is likely to occur. The porated states can be stable themselves, but they can also be transient structures in the translocation pathway. In that case, once enough peptides are adsorbed at the opposing monolayer leaflet, the pores seal. On the other hand, increased accumulation of certain peptides may lead to a detergent-like disintegration of the membrane resulting in formation of non-lamellar, e.g. micellar, systems (solubilization pathway). Note that the secondary structure of the peptides could vary along the various pathways. The helical or random configurations drawn here are merely illustrative of these processes and should not be taken literally.

In recent molecular dynamics (MD) simulations [14] of magainin-H2 interacting with dipalmitoylphosphatidylcholine (DPPC) membranes, an alternative to the states described above was observed, namely the disordered toroidal pore. In contrast to the classic model of a toroidal pore, in the MD study typically only one peptide was found near the pore center, while the other peptides remained close to the pore edge [14]. The disordered toroidal pore model is reminiscent of the micelle-like aggregate model proposed previously [15], which also predicted that the inside of the pore would not be well structured. Although as yet only observed in simulations, it is plausible that the disordered toroidal pore is formed by AMPs in general. Compared to the barrel-stave and traditional toroidal pore models, the disordered toroidal pore has higher entropy, which may lower its overall free energy with respect to the more ordered states. The disordered toroidal pore could either represent a thermodynamically stable state or be an intermediate in the carpet or toroidal pathway. The disordered toroidal pore based on the results of the simulations, has already been used successfully to interpret NMR data on pleurocidin [16], and fluorescence measurements of the cell penetrating peptide Tp-10 [17]. To further explore the structural characteristics of peptide induced pores in detail the original MD simulation techniques, applied to magainin, have been extended to other classes of AMPs.

The focus of the current study is melittin, the major component of bee venom. Melittin has been extensively studied by both experimental and simulation methods. It is a 26-residue cationic polypeptide that has been shown to have hemolytic, antimicrobial and bilayer fusion activity [1,18]. Melittin is unstructured in solution [8] but adopts an α-helical structure when bound to lipid bilayers [12,19–21]. In the membrane, melittin has been postulated to be oriented parallel to the surface of the membrane at low peptide concentration but

insert into the membrane at higher peptide concentrations [22]. It has been proposed that melittin induces toroidal-shaped pores [23,24]. The pore forming propensity of melittin is high in saturated phosphatidylcholine lipids [24,25] and decreases in the presence of negatively-charged [25–27] and polyunsaturated [28] lipids. Pore sizes ranging from 1.5 nm to 5 nm have been reported [11,24,29]. At higher concentrations [12,30] melittin disrupts the bilayer presumably via a carpet mechanism. A recent review [31] provides further insight into other aspects of melittin action.

Previous MD simulations of melittin have shown that when adsorbed on the bilayer surface melittin affects both leaflets of the membrane causing thinning of the upper layer, which in turn favors water penetration through the lower layer [32]. Bachar and Becker [33] reported simulations of a single melittin molecule inserted in a DPPC bilayer in a transmembrane orientation and observed local disorder of the lipids in vicinity of the peptide. In a simulation of a melittin pore, when the individual helices were arranged in a pre-assembled tetrameric aggregate they repelled each other causing a disruption of the lipid bilayer within 4 ns [34]. Whether this represents a realistic description of the mechanism of cytolytic activity of melittin or is due to simulation artifacts has been questioned [35]. Comparisons of simulations of melittin in water, methanol and a dimyristoylphosphatidylcholine (DMPC) bilayer showed that in water and methanol solution melittin is observed to partly unfold, while the peptide retains its structure when embedded in a lipid bilayer [35]. For a more general overview of simulation studies of AMP peptides interacting with lipid bilayers see [36].

Here, we present the results of atomistic MD simulations of melittin interacting with a DPPC bilayer. A range of peptide/lipid (P/L) ratios from 1/128 to 6/128 has been simulated. The approach is similar to our

previous study on magainin peptides [14]. We show that melittin, like magainin, forms disordered toroidal pores in DPPC membranes. To elucidate the role of charges, the process of pore formation in the presence and absence of counter ions has been compared. The effect of the charge state of the basic amino-acid residues on pore formation has also been examined. Finally, simulations of model peptides, not expected to form pores, have been performed to provide a negative control.

2. Methods

2.1. System setup

2.1.1. Melittin/DPPC

A series of simulations of melittin (GIGAVLKVLTTGLPALISWIK-RKRQQ) interacting with DPPC bilayers were performed (see Table 1 for overview). The main system simulated consisted of multiple copies (1–6) of melittin, 128 DPPC lipids, and about 8000 water molecules (the actual number varied depending on the number of peptides). Additional simulations were performed with 8 copies of melittin in a simulation box containing 512 DPPC lipids and about 24,000 water molecules. Initially, each melittin peptide was placed in an α-helical configuration (PDB code: 2MLT [37]) in the water phase close to one of the leaflets of an equilibrated DPPC bilayer. However, in a few simulations, some peptides crossed the water layer and peptides were bound to both leaflets of the membrane. To test the importance of peptide association after binding to the membrane, we also created starting structures from multiple copies of a pre-equilibrated system containing a single surface bound melittin.

2.1.2. Modified electrostatics

Charge-neutral systems containing 4 copies of the peptide, and chloride counter ions were also simulated. In addition, the charges in the peptide were modified by reducing the charges on the amine group of the lysine residues and the guanidinium moiety of the arginine residues to zero. The magainin-H2 peptide was taken from a previous study [14] and 4 copies of the charge-modified system were placed in the simulation box.

2.1.3. Control systems

Control simulations were performed using 4 copies of 20-residue WALP [38] and KALP [39] peptides respectively. WALP and KALP peptides consist of alternating alanine and leucine residues flanked by tryptophan and lysine residues respectively. Experiments show that these peptides insert in a transmembrane orientation, without causing membrane leakage. The KALP and WALP peptides were modeled as ideal helices ($\phi=-57°$, $\psi=-47°$).

2.2. Simulation parameters

2.2.1. Force field

The GROMACS software package [40] was used to perform all the MD simulations. The force field for DPPC was taken from a previous study (setup F) [41]. The GROMOS force field 43a2 [42] was used to describe the peptide interactions and has been used earlier to study similar systems [14]. Both force fields were parameterized for use with a group-based twin range cut-off scheme (using cutoffs of 1.0/1.4 nm and a pair-list update frequency of once per 10 steps) including a reaction field (RF) correction [43] with a dielectric correction of 78 to account for the truncation of long-range electrostatic interactions. Pore formation in simulations where the long-range electrostatics is either treated with particle-mesh Ewald (PME) or RF have been found to be similar but longer time scales are needed with PME [44]. The pores formed in this study using RF were also found to be stable with PME. The water was described using the SPC model [45]. A time step of 2 fs was used. Bond lengths were constrained using the LINCS algorithm [46]. Multiple simulations were performed for each system, starting from different initial Maxwell distributions of random velocities. Most systems were simulated between 50 and 200 ns, depending on when, and if, a pore formed.

2.2.2. State conditions

The simulations were performed in the $NP_lP_z\,T$ ensemble using periodic boundary conditions. The temperature was weakly coupled (coupling time 0.1 ps) to $T=323$ K using a Berendsen thermostat [47]. This temperature is above the main-phase transition temperature of DPPC, experimentally as well as in the model (gel phase formation on the sub-microsecond time scale is only observed for temperatures below 300 K [48]). The pressure was also weakly coupled (coupling time 1.0 ps, compressibility $5*10^{-5}$ bar^{-1}) using a semi-isotropic coupling scheme in which the lateral (P_l) and perpendicular (P_z) pressures are coupled independently at 1 bar [47], corresponding to a tension-free state of the membrane. The simulation setup applied is very similar to that used previously in studies of magainin [14].

2.3. Analysis

2.3.1. Detection and size of pores

The presence of a transmembrane pore was defined by a clustering method, in which only the atomic coordinates of the phosphate atoms of the DPPC molecules were considered. In a bilayer, the phosphate atoms cluster in two groups, namely the two leaflets. However, in the presence of a pore lined by the lipid head-groups, i.e. a toroidal pore, the phosphate atoms cluster as one group. The onset of the pore state was defined as the time when the phosphate atoms cluster as one group. Two phosphate atoms are considered to be in the same cluster if the distance between them is less than the cut-off distance. An adequate cut-off distance for the clustering was found to be 1.2 nm. The

Table 1
An overview of the MD simulations performed

No.	System	Peptides/lipid	Remarks	Time	Association
1	Melittin	1/128	No pore	50 ns	Monomer
2	Melittin	1/128	No pore	100 ns	Monomer
3	Melittin	2/128	No pore	50 ns	Dimer
4	Melittin	2/128	No pore	80 ns	Dimer
5	Melittin	3/128	No pore	175 ns	Trimer
6	Melittin	3/128	Pore	175 ns	Trimer
7	Melittin	3/128	No pore	175 ns	Dimer
8	Melittin	3/128	No pore	175 ns	Trimer
9	Melittin	4/128	Pore	75 ns	Trimer
10	Melittin	4/128	No pore	100 ns	Dimer
11	Melittin	4/128	No pore	100 ns	Trimer
12	Melittin	4/128	Pore	60 ns	Tetramer
13	Melittin	6*/128	No pore	75 ns	Trimer
14	Melittin	6*/128	Pore	50 ns	Tetramer
15	Melittin	6*/128	No pore	45 ns	Trimer
16	Melittin	8*/512	No pore	30 ns	Trimer
17	Melittin	8*/512	Pore	10 ns	Pentamer
18	Melittin	8*/512	Pore	15 ns	Hexamer
19	Melittin + Counter ions	4/128	No pore	140 ns	Dimer
20	Melittin + Counter ions	4/128	Pore	150 ns	Trimer
21	Melittin + Counter ions	4*/128	Pore	200 ns	Trimer
22	Melittin-modified charges	4/128	No pore	50 ns	Trimer
23	Melittin-modified charges	4/128	No pore	50 ns	Tetramer
24	Magainin-modified charges	4/128	No pore	50 ns	Tetramer
25	Melittin-surface bound	4/92	Pore	50 ns	Tetramer
26	WALP	4/128	No pore	100 ns	Trimer
27	WALP	4/128	No epore	100 ns	Tetramer
28	KALP	4/128	No pore	50 ns	Dimer
29	KALP	4/128	No pore	50 ns	Tetramer

Simulations of melittin, magainin-H2, WALP and KALP peptides (column-2) interacting with DPPC bilayers were performed. The number of peptides and lipids in the simulation box is given in column-3. The presence of a pore at the end of the simulation is given in column-4. The lengths of the simulations are given in column-5. The number of peptides in the largest peptide aggregate in the simulation is given in column-6. In the simulations marked with an asterisk, peptides bound to both leaflets of the bilayer.

size of the pore was estimated from the diameter of a circle fitted to the lateral projected density of the glycerol/water interface of the pore.

2.3.2. Peptide helicity

The helicity of the peptides was determined using the DSSP criteria [49]. The total helical content was calculated as the sum of turns and α-helices.

2.3.3. Membrane properties

The lipid bilayer was characterized by analyzing the thickness of the membrane, fluctuations in the thickness of the membrane and the order parameters of the lipid tails. The thickness of the membrane was defined as the average phosphate–phosphate distance during the preporated state. Fluctuations in the thickness were calculated as the standard deviation of the position of the phosphate atoms in the direction perpendicular to the membrane plane. Lipid tail order parameters (S_{CD}) were computed with respect to the membrane normal axis [50].

3. Results and discussion

3.1. Toroidal pores are disordered

A series of atomistic MD simulations of melittin peptides, interacting with a zwitterionic DPPC bilayer was performed an overview of which is provided in Table 1. Starting with peptides initially placed randomly in the solution, the spontaneous formation of transmembrane water pores was observed repeatedly. In the pore state, the lipids bend into the bilayer to continuously line the water pore in a toroidal shape. Similar pore structures are also observed in simulations of lipid membranes interacting with surfactants [51,52], indicating that this type of pore is quite general and can be induced not only by peptides but also by other compounds. Whereas surfactants are able to mix homogeneously with the lipids inside the pore, the peptides do not. Only one or two peptides actually insert into the pore. The remaining peptides line the mouth of the pore, stabilizing its curvature. No regular packing of the peptides is observed, however. Rather, the peptide/lipid pore complex is intrinsically disordered. A snapshot of the disordered toroidal pore is given in Fig. 2, together with a cartoon image comparing the disordered toroidal pore to the traditional model. The arrangement of the melittin peptides and lipids within the pore is similar to that seen previously in the case of magainin-H2 [14]. A striking characteristic of the disordered toroidal pore is that the orientations of the peptides are not well defined. The helical stretches of one or two peptides orient along the membrane normal with a tilt of 45°–90° with respect to the surface of the membrane. Interestingly, the charged residues at the C-terminal end of the peptide were observed to point either into the toroidal pore or towards the water layer. The remaining peptides line the mouth of the pore, with a tilt of 5°–20°. This in line with solid-state NMR data on a synthetic peptide MSI-794, derived from melittin, that suggests that the peptides are oriented nearly parallel to the surface of the bilayer even at concentrations at which pores are induced [53].

The disordered toroidal pore contains on average 8–10 lipid head-groups with an internal diameter of about 1.5 nm. The rim of the pore is about 0.5–1 nm wider. These values lie at the lower end of the experimentally-estimated pore sizes ranging from 1.5 nm to 5 nm [11,24,29]. The variation in the estimates of pore size from dye leakage-experiments could be related to cooperative effects leading to the perturbation of the toroidal pore by the dyes used in the experiments.

In contrast to classical models for toroidal pores, the disordered toroidal pore shows little evidence of structural organization. Similar irregular arrangements have also been reported recently for related peptides [16,17]. The classical model for a toroidal pore was based on the assumption that the pore was cylindrical and that the peptides were oriented in one of the two-states (parallel/perpendicular) [4]. An alternate kinetic model that has been used to reinterpret the experimental data and which matches the simulation results has been proposed [54]. In this model, termed the chaotic or non-stoichiometric pore model, the peptides are not required to line the pore, though a fraction of them may be within the pore. In this model, the arrangement of the peptides in the pore is disorganized and peptides are able to bind on the surface of the membrane even in the presence of a pore. The model has been proposed to be generally applicable [55].

3.2. Multistep pore formation process

In this section, the process by which the peptides porate the membrane is analyzed in detail. Four steps in the process of pore formation can be distinguished.

3.2.1. Step I— membrane binding

In all simulations, the melittin peptides which are initially placed randomly in solution move rapidly (within 5 ns) towards the membrane and bind to the water–lipid interface. Upon binding to the membrane, the peptides orient such that the hydrophilic side-chains of the peptide at the C-terminus interact with the phosphate groups. The hydrophobic N-terminus of the peptide interacts either with the membrane core or with another peptide.
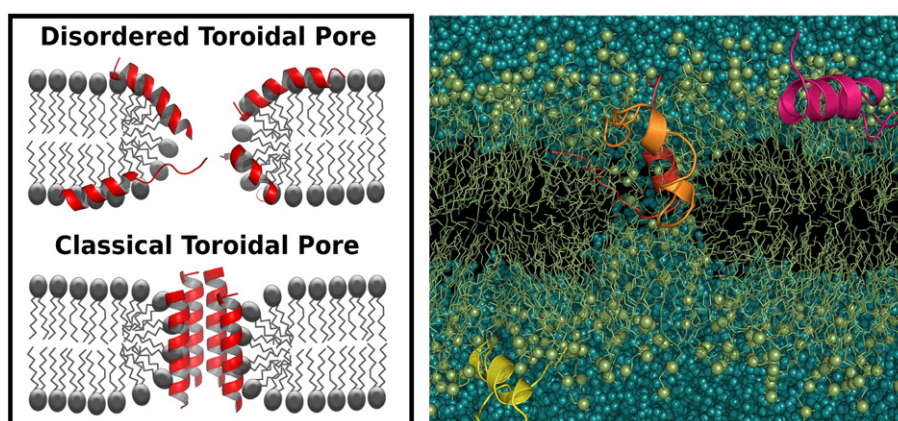

Fig. 2. (Left) A cartoon image comparing the disordered toroidal pore state to the traditional view. A striking characteristic of the disordered toroidal pore is the lack of a well defined peptide orientation as opposed to ordered, transmembrane helices in the classic toroidal pore model. (Right) A snapshot of the disordered toroidal pore from our simulations (simulation 21–200 ns).
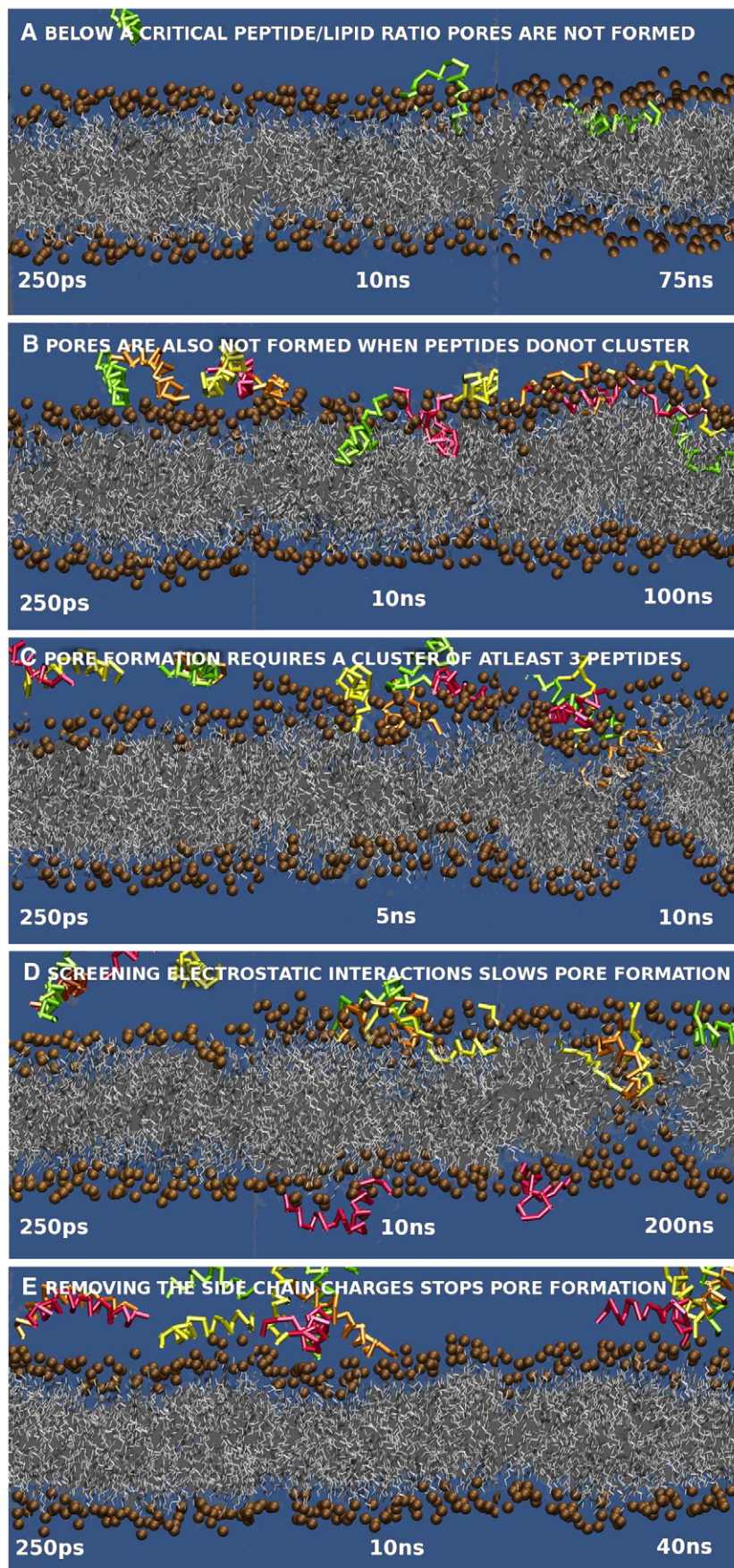
3.2.2. Step II— aggregation

Where only a single peptide is bound to the interface no pore is formed. Pore formation is only observed when the peptides are able to aggregate. This can happen either prior to or concomitant with membrane binding, in the aqueous phase (within 10 ns), or after the peptides have bound to the membrane (10–200 ns). The importance of aggregation is discussed in Section 3.4.

3.2.3. Step III— embedding

After having aggregated, some of the peptides (usually one or two) begin to embed deeper into the interface. This appears to be a cooperative process resulting from the interaction of the peptide aggregate with the lipid head-groups. Electrostatic interactions appear especially important in driving this process (see Section 3.7). The embedding of the peptides causes large deviations from planarity in the leaflet to which peptides are bound and increased fluctuations of the lipid head-groups with respect to the membrane normal (see Section 3.6).

3.2.4. Step IV— pore opening and relaxation

The final step in the process occurs when one of the most deeply embedded peptides connects with the other interface. A water pore forms and one or more peptides together with some lipid molecules move across the membrane causing the pore to relax into a toroidal shape with the structural characteristics described above.

The sequence of events for a specific simulation, Sim 12 is shown in Fig. 3C as an example. The same basic sequence of events i.e., binding and aggregation of the peptides at the interface, the initial embedding of a single peptide deep within the bilayer and increased structural fluctuations leading to translocation and relaxation to a toroidal pore was observed in 9 independent simulations (see Table 1). The time scale required for the formation of a pore was found to vary considerably between different simulations. The time required for pore formation varied between 10 and 200 ns, indicating that it is a stochastic event. In Sim 6, pore formation takes significantly longer as opposed to Sim 12. Pore formation is not always observed in our simulations (see Table 1). In fact, two conditions need to be fulfilled simultaneously in order to trigger pore formation on the time scale accessible to simulations. These conditions are: i) a minimum P/L ratio, and ii) a multimeric peptide aggregate. These conditions are discussed in more detail below.

3.3. A minimum P/L ratio is required to form pores

Transmembrane toroidal pores did not form in simulations with $P/L<1/64$ indicating that spontaneous pore formation requires a minimum P/L ratio. Experimentally, melittin induces the formation of pores in PC vesicles above a specific threshold concentration of $P/L>1/60$ [1]. While this is similar to the concentration at which pore formation was observed in the simulations ($P/L=1/64$), a direct comparison is not possible since local fluctuations in concentration possible in macroscopic systems are absent in the microscopic simulation box. We can also not rule out the possibility that pores form on time scales beyond those accessible in the simulations. Nevertheless, pore formation in the simulations, like in experiment, requires a certain threshold concentration. An example of the time course of events when $P/L=128$, below the threshold ratio, is given in Fig. 3A.

3.4 Peptide aggregation favors pore formation

The aggregation of peptides leading to a high local concentration of the peptides at the membrane surface is also required for pores to form. The simulations presented here, indicate that an aggregate involving at least three peptides is required for pore formation. Fig. 3B shows snapshots from Sim 11 in which the peptides did not associate and there was no pore formation. In contrast, in Sim 10 and Sim 12 (Fig. 3C) where the peptides associated in solution a pore was induced. The results suggest that the pre-association of the peptides, may increase pore propensity as shown experimentally using tetravalent magainin peptides [56].

Interestingly, no specific arrangement of the peptides could be identified within the pore forming peptide aggregates. The peptides generally associated via their aliphatic residues. Association appears to be non-specific and a large number of alternate forms (trimers up to hexamers) induced pore formation. In principle, peptide aggregation leading to pore formation could occur prior or post membrane binding. In the simulations, aggregation of the peptides usually occurred when the peptides were still in the aqueous phase. Once bound the mobility of the peptides at the interface is greatly reduced compared to the water phase. An additional simulation with an increased P/L ratio, in which the peptides were embedded at the interface in monomeric form, shows that peptide aggregation can occur after binding. In this simulation (Table 1-25), the membrane bound peptides aggregated, albeit on a time scale significantly longer than that required in solution. After their association a pore was again formed.

3.5. A helical conformation is not required for pore formation

In all simulations, a significant loss of helicity is observed. Initially, the peptides were placed in solution in a fully helical conformation. In general, unfolding took place while the peptides were still in the aqueous phase in agreement with experimental data [8]. Once bound to the membrane, the average helicity of the melittin peptides was about 40–50%. The helicity is somewhat lower than reported in experiments, which suggest that melittin adopts about 70% alpha-helical conformation when bound to negatively-charged lipids and above 50% when bound to neutral lipids [21]. The loss of helicity was higher in the N-terminal region that is more hydrophobic than the C-terminal region. It is possible that folding of the peptides requires longer time scales than those considered in the simulations (hundreds of nanoseconds). However, it is clear that α-helicity is not a prerequisite for pore formation. Related peptides with varying α-helicity have been shown to have comparable antimicrobial activity [53]. We note that it has been postulated that helicity is required for hemolytic but not antimicrobial activity [57].

3.6. Increased membrane fluctuations and disorder are linked to pore formation

The importance of fluctuations in the thickness of the bilayer for the process of pore formation is illustrated in Fig. 4. Here the deviation from planarity of the DPPC bilayers as a function of peptide concentration is shown. These fluctuations reflect both the rippling of the bilayer plane as a whole and the out-of-plane fluctuations of a few isolated phospholipids. The data corresponds to the period that the bilayer is intact (i.e. before the formation of a pore). At low melittin concentration, the fluctuations in the peptide-free leaflet are small, and comparable to those in the absence of melittin. The fluctuations are significantly larger in the leaflet to which melittin binds. As the concentration of melittin is increased the fluctuations in the bilayer also increase. The fluctuations in the peptide-free leaflet however always remain smaller than in the peptide-bound leaflet.

Fig. 3. Snapshots of the sequence of events in our simulations. A: When less than three peptides are placed in the simulation box, the peptides bind to the interface and do not form a pore (simulation 2). B: Pores are also not formed in the absence of peptide aggregation (simulation 10). C: When three or more peptides ($P/L>60$) are present, the peptides associate and organize to form a poration pathway (simulation 12). D: In the presence of counter ions, pores are formed slower (simulation 21). E: Pores are not formed if the charges on the peptide side-chains are removed (simulation 23).
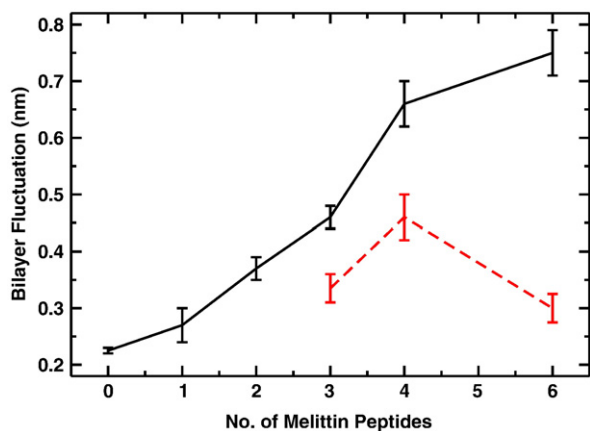
Fig. 4. Fluctuations measured in the planarity of the bilayer as a function of peptide concentration (black). The fluctuation is calculated as the standard deviation of the z coordinate of the phosphate atom of a DPPC molecule. Fluctuation of the peptide-free and non-aggregated peptide-bound leaflets is shown in red.

Interestingly, the fluctuations do not increase linearly with the P/L ratio. The presence of a critical threshold P/L ratio above which these peptides form pores may be responsible for the non-linear response. It has been shown previously that in lipid bilayers flip-flop from one leaflet to the other occurs via a water channel [58]. Thus, dragging the head-groups of a phospholipid from its equilibrium position at the interface into the center of the membrane causes pore formation. The fluctuations that occur in the presence of melittin in effect drag the head-groups towards the interior of the membrane. It is therefore possible that by enhancing these bilayer fluctuations melittin peptides could help overcome the barrier to pore formation.

In contrast to the fluctuations in bilayer thickness, there is little change in the average thickness of the bilayer on peptide binding. The average phosphate–phosphate distance was system dependent but remained close to 3.8 nm (data not shown). However, local thinning of the bilayer was observed since the head-groups close to the peptides deviated from the bilayer plane and embedded deeper within the membrane. A small decrease in thickness, between 0.1 and 0.2 nm, has been reported for the binding of melittin to DOPC membranes [59]. Interestingly, local bilayer thinning of up to 1 nm has been reported for a related antimicrobial peptide MSI-78 in DMPC bilayers [60]. A similar trend was observed for the lipid order parameters in our simulations. The presence of melittin does not substantially change the order of the lipid-chains in the bilayer (averaged over the whole bilayer) compared to a pure DPPC bilayer but it does decrease the order locally. Fig. 5 shows the order parameter profile for lipid tails prior to pore formation. Three groups of lipids are distinguished, namely those in the peptide-free leaflet, lipids in direct contact with the peptides and lipids in the peptide-bound leaflet but not in direct contact with any of the peptides. Averaged over the two leaflets (peptide-bound and peptide-free) the total order of the lipids does not change significantly. However, differences in membrane order are seen between the lipid molecules bound to the peptide and those further away. The close proximity to melittin in the bilayer results in a decrease in the order of the lipids tails compared to the peptide-free bilayer. However, while the lipid molecules directly associated with the peptide have lower order, the lipids away from the peptide become more ordered compensating for the expansion caused by the disordered lipids. The net effect is that the average order of both leaflets is comparable and similar to that in a peptide-free bilayer.

Surprisingly, the area per lipid of the peptide-free leaflet decreased compared to a peptide-free bilayer in the presence of melittin. The marginal decrease in the area per lipid is due to two opposing effects, namely, the expansion of the membrane due to the excluded volume

of the membrane bound peptides and the contraction of the membrane caused by the rippling of one the bilayer leaflets in a finite-sized system. The area per lipid of a pure DPPC bilayer under comparable conditions is 0.68 nm². The value is higher than the experimentally-determined area per lipid due to the high hydration of the system [61]. Upon peptide binding, the area per lipid of the peptide-free bilayer drops by 0.01–0.04 nm². No correlation was found between the decrease in the area per lipid and the peptide concentration but it depended on the degree of rippling and the orientation of the peptides. The observation that, in their membrane bound state prior to pore formation, peptides decrease the order of the adjacent lipids and increase the fluctuation in the bilayer thickness is in agreement with the results obtained for magainin [14].

3.7. Electrostatic interactions are important for pore formation

It has been previously reported that the formation of a water pore can be induced by an asymmetric ion distribution across the membrane [62,63] or an applied electric field [64]. The positively-charged residues in melittin have been implicated to be important for its action [31] and it is possible that the high charge density on the membrane surface may induce pores similar to electroporation by inducing an asymmetric charge distribution.

To test the significance of electrostatic interactions on the process of pore formation by melittin peptides, a series of simulations were performed in which chloride counter ions were added to neutralize the net positive charge of the melittin peptides. It was found that the addition of counter ions increased the time required for the peptides to embed in the membrane to about 10 ns. In addition, at short time scales (up to 20 ns), the peptides inserted less deeply into the membrane compared with simulations performed in the absence of counter ions. Eventually, however, a sequence of events similar to that reported above was observed leading to the formation of a water pore. The time course of pore formation in simulation 21 is shown in Fig. 3D. The counter ions remain distributed throughout the aqueous phase and do not bind to the charged residues. The ions entered the water pore but no actual crossing of the membrane was observed. The stability of water pores in pure DPPC bilayers has been previously shown to be greatly reduced by the presence of the ions due to an increase in pore line tension [44]. This increase in line tension may also be responsible for the decrease in the propensity of the membrane to rupture. Simulations were also performed with either four melittin or four magainin peptides with the charges on the lysine and arginine side-chains removed. The peptides tend to aggregate in clusters that bind loosely to the lipid bilayer. No pore formation event
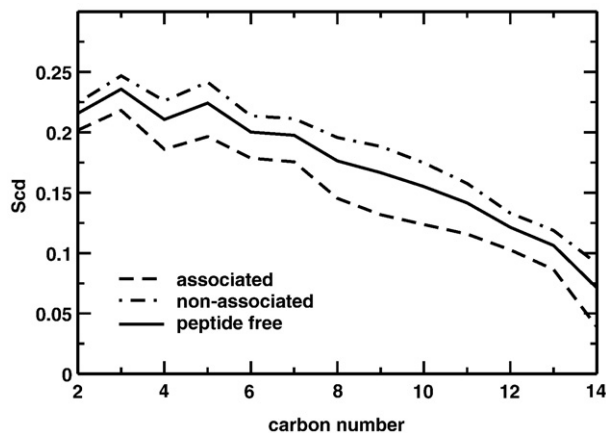

Fig. 5. Lipid tail order parameters of the Sn2 chain obtained from a simulation with four peptides bound to the interface. The order parameters are plotted for lipids in the peptide-free monolayer (—) and in the monolayer to which the peptides bind, divided between peptide-associated (.-.) and non-associated lipids (---).
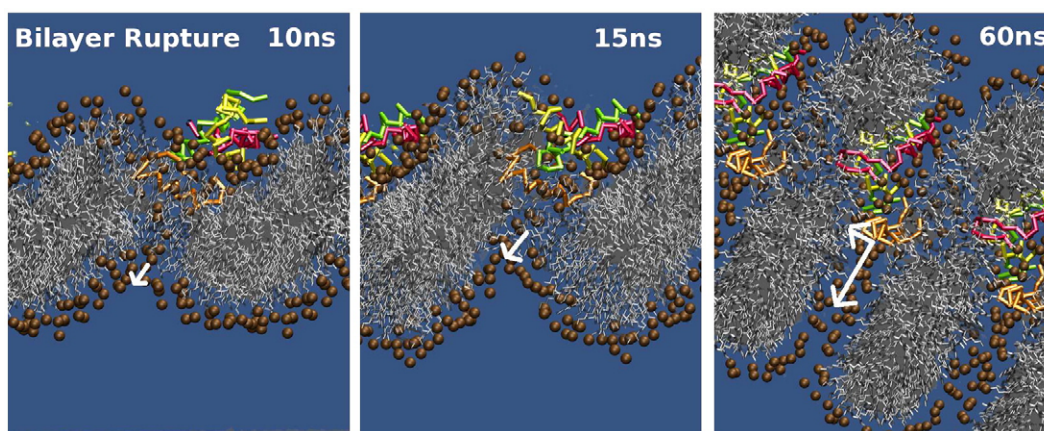
Fig. 6. A recursive mechanism for membrane rupture coined the 'Droste' mechanism. Instead of widening, the pore starts to elongate, dragging additional lipids from the interface to line the pore (left). The drift of lipids from the bilayer toward the pore results in a shrinking of the unperturbed bilayer, up to a point where the melittin peptides which are embedded inside the pore sense the presence of the periodic image of the pore (center). At this point, the pore formation process starts again; a toroidal pore is formed which now connects the original pore to its periodic image (right). This process can, in principle, repeat itself in a recursive scheme until the bilayer is completely destabilized.

was observed in three independent trials (Sims 22–24), although the peptides did form trimeric or tetrameric aggregates (see Fig. 3E).

In summary, the results point to the importance of electrostatic interactions in the poration process. Removing the charges of the basic amino-acid residues of melittin blocks pore formation, while the presence of counter ions lowers the pore forming propensity.

3.8. Membrane rupture via the 'Droste' mechanism

The pores formed in the simulations in which no counter ions were present were not stable. At long time scales the peptides disrupt the bilayer leading to formation of stacked bicellar systems. In this regard the results differ to the stable pores formed in the magainin simulations [14], in which also no counter ions were present. Melittin-induced permeabilization of membranes is known to cause the breakdown of membranes into micelles at high peptide concentrations [12]. Reorganization of lipid assemblies which include permeabilization of multilamellar samples into small vesicles, the fusion of these lipid vesicles to form larger structures and ultimately the fragmentation into discs and micelles depending on the experimental conditions have all been reported [31,65,66].

The mechanism by which the peptides disrupt the membrane in our simulations is illustrated in Fig. 6 which shows snapshots from Sim 12. Specifically, the pore starts to elongate, dragging additional lipids from the interface to line the pore (left). The drift of lipids from the bilayer toward the pore results in the unperturbed bilayer shrinking to the point where the melittin peptides, which are embedded inside the pore feel the periodic image of the pore (center). At this point, the process of pore formation is again initiated and a toroidal pore is formed which now connects the original pore to its periodic image (right). This process can in principle be propagated until the bilayer separates forming micelles. As far as we are aware, such a mechanism for membrane rupture has not been proposed previously. We will use the term 'Droste' mechanism to describe this process of recursive poration in reference to the Droste effect in recursive images. The Droste effect is originally named after a particular recursive image that appeared on the tins and boxes of Droste cocoa powder, one of the main Dutch chocolate producing brands. Whether the Droste mechanism can explain peptide induced membrane rupture in vitro deserves study. Clearly, in the simulations the Droste mechanism is facilitated by the limited size of the system and the application of periodic boundary conditions. However, in real systems at high peptide concentrations multiple transmembrane pores would appear. If the overall pore density is high enough, or if the pores cluster, the peptides could induce a

series of connecting pores similar to that observed in the simulations. We note that a similar deformation of the bilayer has also been observed in simulations of resorcinolic surfactants incorporating into lipid bilayers [52]. The Droste mechanism could therefore be a general mechanism for the disruption of lipid bilayers.

3.9. Non-antimicrobial peptides do not form pores in membranes

Both the WALP [38] (peptides with alternating alanine and leucine residues with flanking tryptophan residues) and KALP [39] (peptides with alternating alanine and leucine residues with flanking lysine residues) peptides have been proposed to adopt a transmembrane orientation in lipid bilayers without the tendency to form pores. Four copies of each these peptides were simulated under the same conditions as described above as control. The peptides are observed to aggregate in water and bind to the membrane. The membrane-absorbed phase appears to be quite stable and the peptides do not penetrate the membrane within 100 ns of simulation. The failure of the peptides to adopt a transmembrane orientation is presumably due to the high barriers to insertion. The differences between the WALP and KALP systems were evident, however. The KALP peptides bind lower in the membrane than the WALP peptides. Larger fluctuations in the thickness of the bilayer were also observed in the case of KALP. These differences can probably be attributed to increased electrostatic interactions in the case of KALP, which has a net charge of +4 due to the terminal lysine residues. In this respect the KALP peptide resembles many AMPs, which carry typically multiple positive charges. However, as no pore forming event was observed we may conclude that a high charge density alone is insufficient to induce pore formation, and that other properties such as the amphipathicity that most AMPs display are also essential.

4. Conclusions

The mechanism of action of the antimicrobial peptide melittin has been studied in a series of MD simulations. Disordered toroidal pores were shown to form spontaneously on a sub-microsecond time scale. In the disordered toroidal pore, the main toroid of the pore is formed by lipid molecules with the peptides binding primarily to the edge of the pore. In general, only one or two peptides were found to insert into the pore and interact with the head-groups and water molecules. Based on the results of our simulations, we believe that the disordered toroidal pore may be a general mechanism by which small peptides form pores. It has now been observed for multiple systems under a variety of conditions, including different peptide/lipid ratios, the presence or

absence of counter ions, and for different peptides including magainin [14], melittin, and indolicidin (D. Sengupta, work in progress).

The process of pore formation by melittin appears to be cooperative requiring a minimum critical peptide to lipid ratio and a high local peptide concentration or multimeric aggregate. Whether aggregation takes place prior or following membrane binding appears not to affect the thermodynamically preferred pathway though the kinetics of the processes differ. Membrane binding leads to asymmetric changes in the lipid tail order with the lipid molecules bound to the peptides being less ordered while those further away more ordered. Large fluctuations within the membrane precede pore formation and could help overcome the barrier to pore formation. We have shown that the charged residues within the peptide play an important role in driving the system from the membrane bound state to the porated state. Simulations with blocked lysine and arginine charges do not form pores indicating the importance of charged residues in pore formation. Non-antimicrobial peptides, WALP and KALP, simulated under identical conditions did not form pores on the time scale investigated. The presence of counter ions slows the process of pore formation and appears to make the pores more stable. In the absence of counter ions complete membrane rupture is observed via a recursive mechanism. Such a recursive or Droste mechanism might be a general mechanism by which surfactants and peptides solubilize membranes.

Acknowledgments

References

[1] K.A. Brogden, Antimicrobial peptides: pore formers or metabolic inhibitors in bacteria? Nat. Rev. Microbiol. 3 (2005) 238–250.

[2] K.L. Brown, R.E. Hancock, Cationic host defense (antimicrobial) peptides, Curr. Opin. Immunol. 18 (2006) 24–30.

[3] Y. Shai, Mode of action of membrane active antimicrobial peptides, Biopolymers 66 (2002) 236–248.

[4] H.W. Huang, Molecular mechanism of antimicrobial peptides: the origin of cooperativity, Biochim. Biophys. Acta 1758 (2006) 1292–1302.

[5] B. Bechinger, K. Lohner, Detergent-like actions of linear amphipathic cationic antimicrobial peptides, Biochim. Biophys. Acta 1758 (2006) 1529–1539.

[6] L. Stella, C. Mazzuca, M. Venanzi, A. Palleschi, M. Didone, F. Formaggio, C. Toniolo, B. Pispisa, Aggregation and water-membrane partition as major determinants of the activity of the antibiotic peptide Trichogin GA IV, Biophys. J. 86 (2004) 936–945.

[7] D. Raimondo, G. Andreotti, N. Saint, P. Amodeo, G. Renzone, M. Sanseverino, I. Zocchi, G. Molle, A. Motta, A. Scaloni, A folding-dependent mechanism of antimicrobial peptide resistance to degradation unveiled by solution structure of distinctin, Proc. Natl. Acad. Sci. USA. 102 (2005) 6309–6314.

[8] J. Lauterwein, L.R. Brown, K. Wuethrich, High-resolution 1H-NMR studies of monomeric melittin in aqueous solution, Biochim. Biophys. Acta 622 (1980) 219–230.

[9] S. Qian, W. Wang, L. Yang, H.W. Huang, Structure of the alamethicin pore reconstructed by X-ray diffraction analysis, Biophys. J. 94 (2008) 3512–3522.

[10] K. Matsuzaki, K. Sugishita, N. Ishibe, M. Ueha, S. Nakata, K. Miyajima, R.M. Epand, Relationship of membrane curvature to the formation of pores by magainin 2, Biochemistry 37 (1998) 11856–11863.

[11] K. Matsuzaki, S. Yoneyama, K. Miyajima, Pore formation and translocation of melittin, Biophys. J. 73 (1997) 831–838.

[12] A. Naito, T. Nagao, K. Norisada, Mizuno, S. Tuzi, H. Saito, Conformation and dynamics of melittin bound to magnetically oriented lipid bilayers by solid-state 31P and 13C NMR spectroscopy, Biophys. J. 78 (2000) 2405–2417.

[13] A. Pokorny, P.F.F. Almeida, Kinetics of dye efflux and lipid flip-flop induced by D-lysin in phosphatidylcholine vesicles and the mechanism of graded release by amphiphatic, a-helical peptides, Biochemistry 43 (2004) 8846–8857.

[14] H. Leontiadou, A.E. Mark, S.J. Marrink, Antimicrobial peptides in action, J. Am. Chem. Soc. 128 (2006) 12156–12161.

[15] R.E.W. Hancock, D.S. Chapple, Peptide antibiotics, Antimicr. Ag. Chemother. 43 (1999) 1317–1323.

[16] A.J. Mason, A. Marquette, B. Bechinger, Zwitterionic phospholipids and sterols modulate antimicrobial peptide induced membrane destabilisation, Biophys. J. 93 (2007) 4289–4299.

[17] L.E. Yandek, A. Pokorny, A. Floren, K. Knoelke, U. Langel, P.F.F. Almeida, Mechanism of the cell-penetrating peptide transportan 10 permeation of lipid bilayers, Biophys. J. 92 (2007) 2434–2444.

[18] C.E. Dempsey, The actions of melittin on membranes, Biochim. Biophys. Acta 1031 (1990) 143–161.

[19] I. Constantinescu, M. Lafleur, Influence of the lipid composition on the kinetics of concerted insertion and folding of melittin in bilayers, Biochim. Biophys. Acta 1667 (2004) 26–37.

[20] H. Vogel, F. Jähnig, The structure of melittin in membranes, Biophys. J. 50 (1986) 573–582.

[21] N. Asthana, S.P. Yadav, J.K. Ghosh, Dissection of antibacterial and toxic activity of melittin: a leucine zipper motif plays a crucial role in determining its hemolytic activity but not antibacterial activity, J. Biol. Chem. 279 (2004) 55042–55050.

[22] K. Hristova, C.E. Dempsey, S.H. White, Structure, location, and lipid perturbations of melittin at the membrane interface, Biophys. J. 80 (2001) 801–811.

[23] D. Allende, S.A. Simon, T.J. McIntosh, Melittin-induced bilayer leakage depends on lipid material properties: evidence for toroidal pores, Biophys. J. 88 (2005) 1828–1837.

[24] L. Yang, T.A. Harroun, T.M. Weiss, L. Ding, H.W. Huang, Barrel-stave model or toroidal model? A case study on melittin pores, Biophys. J. 81 (2001) 1475–1485.

[25] M. Monette, M. Lafleur, Modulation of melittin-induced lysis by surface charge density of membranes, Biophys. J. 68 (1995) 187–195.

[26] D.K. Hincha, J.H. Crowe, The lytic activity of the bee venom peptide melittin is strongly reduced by the presence of negatively charged phospholipids or chloroplast galactolipids in the membranes of phosphatidylcholine large unilamellar vesicles, Biochim. Biophys. Acta 1284 (1996) 162–170.

[27] G. van den Bogaart, J.T. Mika, V.V. Krasnikov, B. Poolman, The lipid dependence of melittin action investigated by dual-color fluorescence burst analysis, Biophys. J. 93 (2007) 154–163.

[28] M. Monette, M. Lafleur, Influence of lipid chain unsaturation on melittin-induced micellization, Biophys. J. 70 (1996) 2195–2202.

[29] A.S. Ladokhin, M.E. Selsted, S.H. White, Sizing membrane pores in lipid vesicles by leakage of co-encapsulated markers: pore formation by melittin, Biophys. J. 72 (1997) 1762–1766.

[30] A.S. Ladokhin, S.H. White, Detergent-like permeabilization of anionic lipid vesicles by melittin, Biochim. Biophys. Acta 1514 (2001) 253–260.

[31] H. Raghuraman, A. Chattopadhyay, Melittin: a membrane-active peptide with diverse functions, Biosci. Rep. 27 (2007) 189–223.

[32] S. Berneche, M. Nina, B. Roux, Molecular dynamics simulation of melittin in a dimyristoylphosphatidylcholine bilayer membrane, Biophys. J. 75 (1998) 1603–1618.

[33] M. Bachar, O.M. Becker, Protein-induced membrane disorder: a molecular dynamics study of melittin in a dipalmitoylphosphatidylcholine bilayer, Biophys. J. 78 (2000) 1359–1375.

[34] J.H. Lin, A. Baumgaertner, Stability of a melittin pore in a lipid bilayer: a molecular dynamics study, Biophys. J. 78 (2000) 1714–1724.

[35] A. Glättli, I. Chandrasekhar, W.F. van Gunsteren, A molecular dynamics study of the beevenom melittin in aqueous solution, in methanol, and inserted in a phospholipid bilayer, Eur. Biophys. J. 35 (2006) 1–13.

[36] E. Matyus, C. Kandt, D.P. Tieleman, Computer simulation of antimicrobial peptides, Curr. Med. Chem. 14 (2007) 2789–2798.

[37] T.C. Terwilliger, D. Eisenberg, The structure of melittin. I. Structure determination and partial refinement, J. Biol. Chem. 257 (1982) 6010–6015.

[38] J.A. Killian, I. Salemink, M.R.R. de Planque, G. Lindblom, R.E. Koeppe, D.V. Greathouse, Induction of nonbilayer structures in diacylphosphatidylcholine model membranes by transmembrane helical peptides: importance of hydrophobic mismatch and proposed role of tryptophans, Biochemistry 35 (1996) 1037–1045.

[39] M.R.R. de Planque, J.A.W. Kruijtzer, R.M.J. Liskamp, D. Marsh, D.V. Greathouse, R.E. K.B. de Kruijff II, J.A. Killian, Different membrane anchoring positions of tryptophan and lysine in synthetic transmembrane a-helical peptides, J. Biol. Chem. 274 (1999) 20839–20846.

[40] D. van der Spoel, E. Lindahl, B. Hess, G. Groenhof, A.E. Mark, H.J.C. Berendsen, GROMACS: fast, flexible, and free, J. Comp. Chem. 26 (2005) 1701–1718.

[41] C. Anezo, A.H. de Vries, H.D. Höltje, D.P. Tieleman, S.J. Marrink, Methodological issues in lipid bilayer simulations, J. Phys. Chem. B 107 (2003) 9424–9433.

[42] W.F. van Gunsteren, X. Daura, A.E. Mark, Encyclopedia of Computational Chemistry, Vol. 2, Wiley and Sons, 1998.

[43] I.G. Tironi, R. Sperb, P.E. Smith, W.F. van Gunsteren, A generalized reaction field method for molecular dynamics simulations, J. Chem. Phys. 102 (1995) 5451–5459.

[44] H. Leontiadou, A.E. Mark, S.J. Marrink, Ion transport across transmembrane pores, Biophys. J. 92 (2007) 4209–4215.

[45] H.J.C. Berendsen, J.P.M. Postma, W.F. van Gunsteren, J. Hermans, Interaction Models for Water in Relation to Protein Hydration, Reidel, Dordrecht, 1981.

[46] B. Hess, H. Bekker, H.J.C. Berendsen, J.G.M. Fraaije, Lincs: a linear constraint solver for molecular simulations, J. Comp. Chem. 18 (1997) 1463–1472.

[47] H.J.C. Berendsen, J.P.M. Postma, W.F. van Gunsteren, A.D. Nola, J.R. Haak, Molecular dynamics with coupling to an external bath, J. Chem. Phys. 81 (1984) 3684–3690.

[48] A.H. de Vries, S. Yefimov, A.E. Mark, S.J. Marrink, Molecular structure of the lecithin ripple phase, Proc. Natl. Acad. Sci. USA. 102 (2005) 5392–5396.

[49] W. Kabsch, C. Sander, Dictionary of protein secondary structure: pattern recognition of hydrogen-bonded and geometrical features, Biopolymers 22 (1983) 2577–2637.

[50] E. Egberts, S.J. Marrink, H.J.C. Berendsen, Molecular dynamics simulation of a phospholipid membrane, Eur. Biophys. J. 22 (1994) 423–436.

[51] A.A. Gurtovenko, J. Anwar, Modulating the structure and properties of cell membranes: the molecular mechanism of action of dimethyl sulfoxide, J. Phys. Chem. B 111 (2007) 10453–10460.

[52] M. Siwko, Disturb or stabilize: the dual effect of resorcinols on lipid membranes, Ph.D. thesis, University of Groningen, 2008.

[53] A. Ramamoorthy, S. Thennarasu, D.-K. Lee, A. Tan, L. Maloy, Solid-state NMR investigation of the membrane-disrupting mechanism of antimicrobial peptides MSI-78 and MSI-594 derived from magainin 2 and melittin, Biophys. J. 91 (2006) 206–216.

[54] S.M. Gregory, A. Cavenaugh, V. Journigan, A. Pokorny, P.F.F. Almeida, A quantitative model for the all-or-none permeabilization of phospholipid vesicles by the antimicrobial peptide Cecropin A, Biophys. J. 94 (2008) 1667–1680.

[55] P.H. Axelsen, A chaotic pore model of polypeptide antibiotic action, Biophys. J. 94 (2008) 1549–1550.

[56] C.J. Arnusch, H. Brandenhorst, B. de Kruijff, R.M.J. Liskamp, E. Breukink, R.J. Pieters, Enhanced membrane pore formation by multimeric/oligomeric antimicrobial peptides, Biochemistry 46 (2007) 13437–13442.

[57] Y. Chen, C.T. Mant, S.W. Farmer, R.E.W. Hancock, M.L. Vasil, R.S. Hodges, Rational design of a-helical antimicrobial peptides with enhanced activities and specificity/therapeutic index, J. Biol. Chem. 280 (2005) 12316–12329.

[58] D.P. Tieleman, S.J. Marrink, Lipids out of equilibrium: energetics of desorption and pore mediated flip-flop, J. Am. Chem. Soc. 128 (2006) 12462–12467.

[59] F. Chen, M. Lee, H.W. Huang, Evidence for membrane thinning effect as the mechanism for peptide-induced pore formation, Biophys. J. 84 (2003) 3751–35758.

[60] A. Mecke, D. Lee, A. Ramamoorthy, B.G. Orr, M.M. Banaszak Holl, Membrane thinning due to antimicrobial peptide binding: an atomic force microscopy study of MSI-78 in lipid bilayers, Biophys. J. 89 (2005) 4043–4050.

[61] J.F. Nagle, R. Zhang, S. Tristram-Nagle, W. Sun, H.I. Petrache, R.M. Suter, X-ray structure determination of fully hydrated La phase dipalmitoylphosphatidylcholine bilayers, Biophys. J. 70 (1996) 1419–1431.

[62] A.A. Gurtovenko, I. Vattulainen, Pore formation coupled to ion transport through lipid membranes as induced by transmembrane ionic charge imbalance: atomistic molecular dynamics study, J. Am. Chem. Soc. 127 (2005) 17570–17571.

[63] L. Delemotte, F. Dehez, W. Treptow, M. Tarek, Modeling membranes under a transmembrane potential, J. Phys. Chem. B 112 (2008) 5547–5550.

[64] D.P. Tieleman, H. Leontiadou, A.E. Mark, S.J. Marrink, Simulation of pore formation in lipid bilayers by mechanical stress and electric fields, J. Am. Chem. Soc. 125 (2003) 6382–6383.

[65] J. Dufourcq, J.F. Faucon, G. Fourche, J.L. Dasseux, M.L. Maire, T. Gulik-Krzywicki, Morphological changes of phosphatidylcholine bilayers induced by melittin: vesicularization, fusion, discoidal particles, Biochim. Biophys. Acta 859 (1986) 33–48.

[66] J.F. Faucon, J.M. Bonmatin, J. Dufourcq, E.J. Dufourc, Acyl chain length dependence in the stability of melittin-phosphatidylcholine complexes. A light scattering and 31P-NMR study, Biochim. Biophys. Acta 1234 (1995) 235–243.